Fizika Nizkikh Temperatur, 2003, v. 29, Nos. 9/10, p. 1118–1124

The vibration-rotation of H_2O and its complexation with CO_2 in solid argon revisited

Xavier Michaut, Anne-Marie Vasserot, and Luce Abouaf-Marguin

Laboratoire de Physique Moléculaire et Applications, UMR CNRS 7092
Université Pierre et Marie Curie, boîte 76, 4 place Jussieu
75252 Paris, Cedex 05, France
E-mail: xmichaut@ccr.jussieu.fr

Fourier-transform infrared spectroscopy in the frequency range 400–4000 cm^{-1} has been used to investigate the absorption of H_2O and H_2O:CO_2 complex isolated in solid argon. Thanks to the lowest temperature reached in our experiment, temperature effects and nuclear spin conversion studies allow us to propose a new assignment of the rovibrational lines in the bending band ν_2 for the quasi-freely rotating H_2O. An additional wide structure observed in this band shows two maxima around 1657.4 and 1661.3 cm^{-1}, with nuclear spin conversion of the high frequency part into the low frequency one. This structure is tentatively attributed to a rotation-translation coupling of the molecule in the cage. However, the equivalent effect is not observed in the vibrational stretching bands ν_1 and ν_3. Finally, by double doping experiments with CO_2, important new structures appear, leading us to unambiguously extract the frequencies of the lines of the H_2O:CO_2 complex.

PACS: 33.15.Mt, 33.20.Ea, 33.20.Vq

1. Introduction

The water molecule is of C_{2v} symmetry. In the gas phase, its rovibrational spectrum is well known up to 26000 cm^{-1} [1–3] and in the solid state, the structures of the different forms of ice have been extensively studied [4–6]. Ice grains play an important role in the chemistry of the interstellar medium and of planetary atmospheres [7,8]. D'Hendecourt et al. [9] have shown from IRAS-LRS observations of protostars, that CO_2 is a wide-spread and very common component of the interstellar medium. The complexes between H_2O and CO_2 have been also the subject of several previous studies [10,11].

It is well known that the matrix isolation technique, combined with IR absorption spectroscopy, remains a powerful tool to study the formation and the geometry of weakly bonded complexes. Before looking at the H_2O:CO_2 complex, pure H_2O in matrices had to be studied under our experimental conditions. Since the work of Glasel [12], all evidence indicates that H_2O trapped in inert matrices, is almost freely rotating [13–17]. After some initial controversies, there is now general agreement on the assignment of the rovibrational absorptions in the ν_2 and ν_1/ν_3 regions in solid argon [16]. This assignment is also very important for all matrix isolation studies because water is a common impurity. In the same way, as CO_2 is also always present as an impurity in matrix experiments, the identification of complexes of water with CO_2 is essential.

In the present paper, we will focus attention on the hindered rotational motion of water molecules in solid argon. After a brief description of the experimental conditions, we will present the calculation of the cold gas transitions. Then, experimental results will be presented including temperature and time effects. An assignment of the lines will be proposed. The last section is devoted to identification of absorption lines of CO_2:H_2O weakly bonded complexes through double doping experiments with CO_2. The results will be discussed in the light of recent data.

2. Experimental

The experimental setup has already been described [18]. We only review here the main and specific features. Ar and CO_2 (L'Air Liquide – 99.995 % and 99.99 % respective purity) are used without purification. Water is deionized, doubly distilled and carefully degassed. The gaseous mixture is obtained by standard manometric procedures. As water is adsorbed

on the walls of the stainless steel part of the sample system, we carefully passivated the system with a pressure of water equal to its partial pressure in the gas mixture. During deposition, we checked that water absorptions were proportional to the amount of deposited gas mixture.

To study weakly bonded complexes, the relative concentrations have to be carefully chosen [19]. For molecules which do not react with each other, as is the present case [10], more than the statistical number of mixed pairs can be obtained by premixing the two molecules with argon in the gas sample [20].

The samples were obtained by the slow spray-on technique (10 mmol/h) of the gaseous mixture onto a gold plated mirror held at 20 K. The solid sample is then cooled to 6 K and annealed at least up to 30 K to allow a reorganization of the polycristalline film (narrowing of the lines) and a migration of molecular species.

Absorption spectroscopy is performed using a Bruker IFS 113V FTIR spectrometer, with a maximum resolution of 0.03 cm^{-1} and, for this resolution, an accuracy better than 0.02 cm^{-1}. Broad lines frequencies are estimated within a 0.1 cm^{-1} precision.

3. Calculation of the «cold» gas transitions

As the rotation is almost free, a comparison with the expected spectrum of the gas at 6 and 20 K is helpful for the transition assignments. The water molecule, C_{2v} symmetry type, is an asymmetric rotor, with two magnetic species, ortho (spin degeneracy 3) and para (spin degeneracy 1). In Fig. 1, the rovibrational transitions are indicated for the three fundamental bands of H_2O, numbered in increasing frequencies of the gas phase. At 20 K, the $J = 0$ and 1 energy levels are the only ones sufficiently populated to give rise to detectable absorptions. If the nuclear spin conversion were fast, for the ν_2 mode, only the para line *4* should appear at 6 K. But, as well known, the conversion is very slow in low temperature matrices [21]. Then *2* other lines, the ortho *3* and *5* ones, remain detectable, as long as Boltzmann population of 20 K is trapped for some time on the 1_{01} ortho level. Using the intensities reported in HITRAN96 data base [1], bar spectra can be calculated at 20 and 6 K (graphs labeled G on Figs. 2).

4. Experimental results in the ν_2 region of H_2O

We will now discuss in detail the ν_2 range and then, give the results obtained with similar arguments for the ν_1 and ν_3 bands. The observed frequencies, measured with 0.03 cm^{-1} maximum resolution are in Table 1, and compared to the most recent literature data [16].

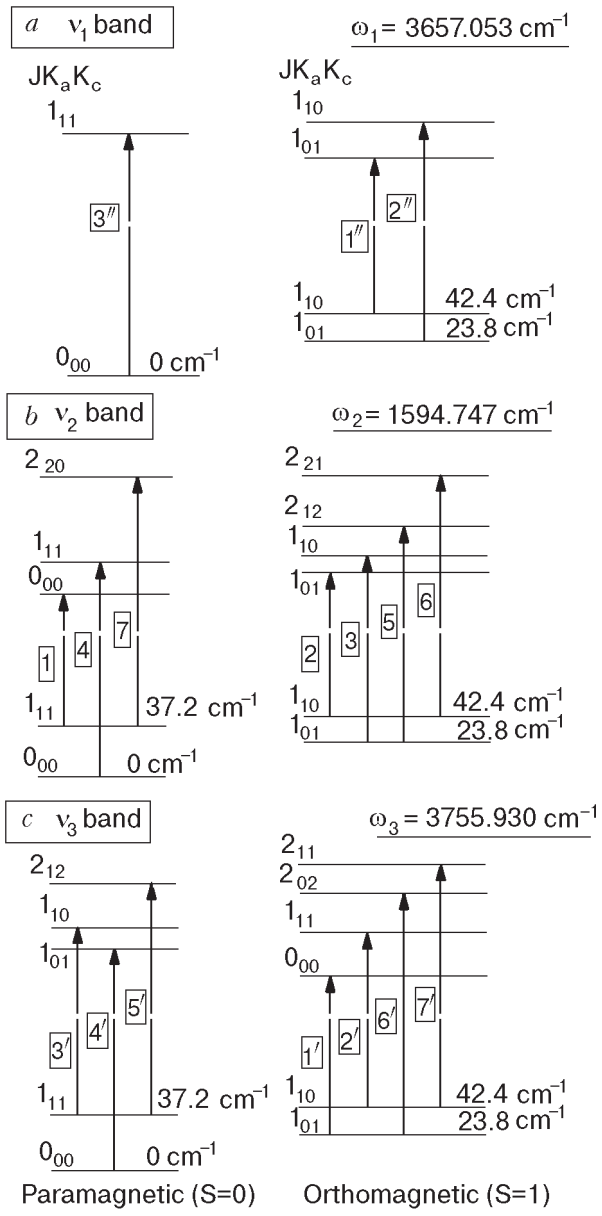

Fig. 1. Rovibrational transitions of the three modes of gaseous H_2O at 20 K: ν_1 band (*a*); ν_2 band (*b*); ν_3 band (*c*); J, K_a, K_c are the rotational quantum numbers of the asymmetric rotator; S is the nuclear spin quantum number.

A typical spectrum of a sample $H_2O/Ar = 1/500$ is presented in Fig. 2 at 20 and 6 K.

Temperature effect

The two lines at 1556.6 and 1573.2 cm^{-1} and the broad structure around 1690 cm^{-1} which appear at 20 K, disappear totally at 6 K. The effect is reversible. By comparison with the gas spectrum, it seems obvious that those structures correspond, respectively, to lines *1*, *2* and *6*/*7*. Intensity comparisons with the gas are also in favor of this interpretation, as it is known that the matrix does not change dramatically the relative intensities of the transitions.

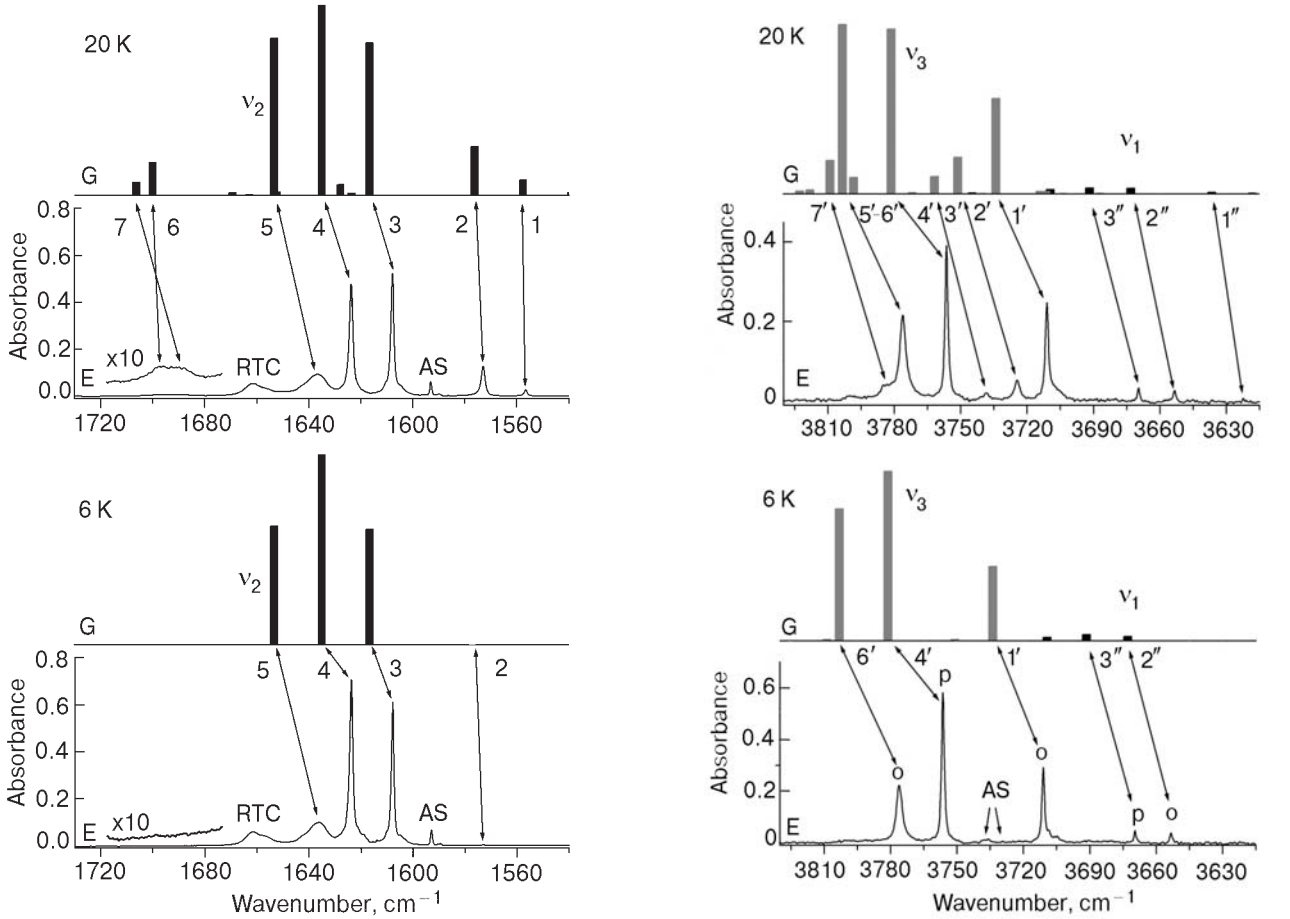

Fig. 2. Spectra at 20 and 6 K of the ν_1, ν_2, ν_3 regions of H_2O. G is the simulated bar spectrum of the gas, the numbers refer to the transitions of Fig. 1; E is the experimental spectrum ($H_2O/Ar = 1/500$) recorded with 0.15 cm^{-1} resolution, just after deposition at 20 K (thickness ~ 250 μm), the arrows indicate the present assignments, RTC is the rotation-translation coupling structure and AS corresponds to the H_2O dimmer; *o* and *p* are orthomagnetic and paramagnetic species.

Table 1

Frequencies (cm^{-1}) and assignments of absorption lines of monomeric H_2O in the ν_2 region in solid argon

Line	Transition	Magnetic species	Gas [1]	This work	Perchard [16]
1	$1_{11}\rightarrow 0_{00}$	para	1557.611	1556.6[a]	1556.7
2	$1_{10}\rightarrow 0_{01}$	ortho	1576.188	1573.2[a]	1573.1
					1589.2[c] (NRM)
3	$1_{01}\rightarrow 1_{10}$	ortho	1616.714	1607.82[b]	1607.9
4	$0_{00}\rightarrow 1_{11}$	para	1634.970	1623.72[b]	1623.8
5	$1_{01}\rightarrow 2_{12}$	ortho	1653.268	1636.3[b]	1636.5
RTC	Rotation translation coupling	para ortho		1657.4[b] 1661.3[b]	
6	$1_{10}\rightarrow 2_{21}$	ortho	1699.935	1697.8[a]	1661.4
7	$1_{11}\rightarrow 2_{20}$	para	1706.355	1689.7[a]	1657.2
					1687.6 1699.9 (Phonon activation)

[a]Measured at 20 K. [b]Measured at 6 K. [c]Nonrotating molecule.

At this point, we would disagree with the conclusions of previous work in solid argon [13–16] which assign lines *6* and *7* to the double structure observed at 1660 cm^{-1}. This does not seem possible since these lines do not start from the lowest energy level. They should disappear at 6 K, as lines *1*, *2* and *6*/*7*, whereas this 1660 cm^{-1} double structure remains. On the other hand, the 1690 cm^{-1} structure appears only when the temperature is raised. Our very recent experiments, at 20 K, with high optical density samples [22], show that in this broad structure at 1690 cm^{-1}, which exhibits clearly two maxima (1689.7 and 1697.8 cm^{-1}), the low frequency maximum decreases much faster than the high frequency one as the temperature is lowered. This low frequency shoulder corresponds then to a transition from a level with a higher energy gap to the fundamental than the high frequency one and should be assigned to line *7*. So the line at 1697.8 cm^{-1} corresponds to transition *6*. Those lines are broad, as the 1636.3 one, compared to lines *2*, *4* and *5*, because they involve a $J = 2$ level which is more affected than levels $J = 0$ or 1 by the coupling to the matrix.

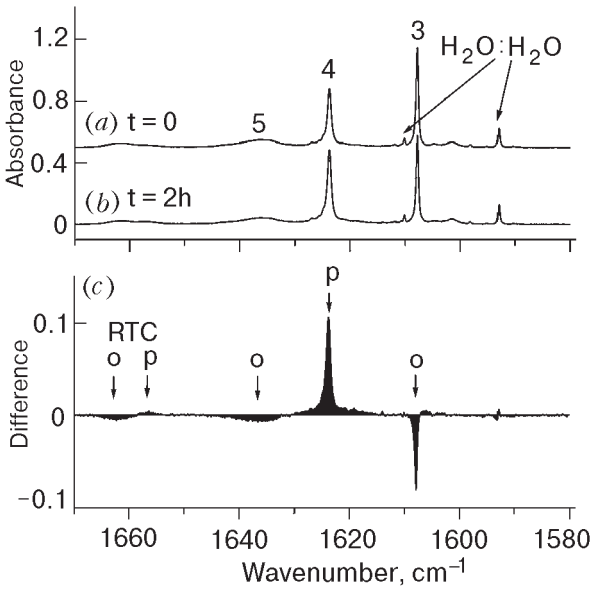

Fig. 3. Time effect in the ν_2 region of H_2O, due to nuclear spin conversion at 6 K. The spectra (H_2O/Ar = 1/1000) are recorded with 0.15 cm^{-1} resolution, after annealing at 30 K (thickness ~ 220 μm) after a time t = 0 (*a*) and 2 (*b*) hours; the numbers refer to the transitions of Fig. 1; (*c*) presents the difference of spectra (*a*) and (*b*), *o* and *p* are orthomagnetic and paramagnetic species.

At 6 K, the 1607.82, 1623.72 and 1636.3 cm^{-1} lines correspond respectively to transitions *3*, *4* and *5* in agreement with previous assignments. Transition *5*, which involves a J = 2 level, is also broad.

So far, there is no obvious assignment for the double structure at 1660 cm^{-1}, which remains at 6 K, does not vanish at 20 K, showing only a weak broadening. By changing the concentrations, and upon annealing, we have checked that its intensity is related to the concentration of the monomer absorbers.

In Fig. 2, one additional line appears at 1592.94 cm^{-1}, which corresponds to the dimer of H_2O, in agreement with previous work as we notice later on Table 3 (see Sec. 6).

Furthermore, the line measured at 1589.2 cm^{-1} [16] may be assigned to nonrotating molecules [13–16]. Whatever our experimental conditions, with samples of pure H_2O, this line was always very weak. In section 6 of this paper, we will show that it is due to the H_2O:CO_2 complex, since CO_2 is generally present as an impurity in the samples.

Time effect

As already mentioned, the nuclear spin conversion from the ortho to the para form is slow in low temperature matrices [21]. The time evolution of the spectra can confirm the assignments, since ortho lines should decrease to the benefit of para lines, when starting from nonequilibrated Boltzmann populations at 6 K. Figure 3 exhibits these intensity changes after two hours. The first spectrum is taken just after a fast cooling from 30 K. Lines *3* and *5* decrease when *4* increases, which is consistent with the assignments. In the double structure near 1660 cm^{-1}, the high frequency part (1661.3 cm^{-1}) decreases and the low frequency one (1657.4 cm^{-1}) increases correlatively. This structure presents an ortho and a para components, is situated between 50 and 100 cm^{-1} far from the pure vibrational frequency and remains at 6 K. It does not belong to the rovibrational structure, but is related to the number of rotating molecules. It may then be a manifestation of the rotation-translation coupling (RTC) involved in the movement of the molecule in its cage [23].

The weak lines at 1592.94 and 1610.12 cm^{-1} are due to dimers (Table 3). The line 1610.12 cm^{-1} is hidden in the high frequency wing of line *3* in Fig. 2 but appears after annealing to 30 K (Fig. 3).

5. Experimental results in the ν_1 and ν_3 regions of H_2O

The 3600–3800 cm^{-1} region is represented in Fig. 2 at 20 and 6 K (H_2O/Ar = 1/500), together with the calculated gaseous bar spectra. With the same arguments as for ν_2, we present the assignments in Table 2, which agree with the most recent work [16].

Table 2

Frequencies (cm^{-1}) and assignments of absorption lines of monomeric H_2O in the ν_1 and ν_3 region in solid argon

Line	Transition	Magnetic species	Gas [1]	This work	Perchard [16]
ν_1 band					
1″	$1_{10}\rightarrow1_{01}$	ortho	3638.082	3622.4[a]	3622.7
					3638.3[c] (NRM)
2″	$1_{01}\rightarrow1_{10}$	ortho	3674.697	3653.38[b]	3653.5
3″	$0_{00}\rightarrow1_{11}$	para	3693.294	3669.85[b]	3669.7
ν_3 band					
1′	$1_{01}\rightarrow0_{00}$	ortho	3732.135	3711.2[a]	3711.3
2′	$1_{10}\rightarrow1_{11}$	ortho	3749.331	3724.7[a]	3724.9
					3736.0[c] (NRM)
3′	$1_{11}\rightarrow1_{10}$	para	3759.845	3739.4[a]	3739.0
4′	$0_{00}\rightarrow1_{01}$	para	3779.493	3756.49[b]	3756.6
6′	$1_{01}\rightarrow2_{02}$	ortho	3801.420	3776.30[b]	3776.4
7′	$1_{10}\rightarrow2_{11}$	ortho	3807.014	3784.5[a]	

[a]Measured at 20 K. [b]Measured at 6 K. [c]Nonrotating molecule.

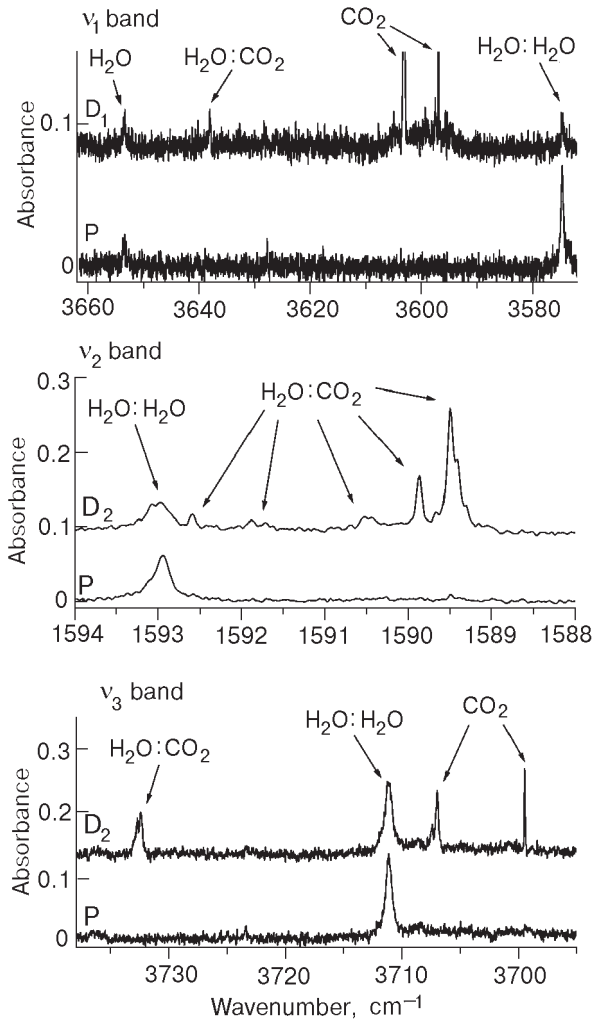

Fig. 4. Double doping with CO_2: water regions at 6 K. The spectra are recorded with 0.03 cm^{-1} resolution, after annealing at 30 K; P is a pure H_2O sample ($H_2O/Ar = 10/5000$, thickness ~ 60 μm); D_1 and D_2 are the double doped samples (D_1: $H_2O/CO_2/Ar = 10/5/5000$, thickness ~ 80 μm; D_2: $H_2O/CO_2/Ar = 10/2/5000$, thickness ~ 60 μm).

However, two points should be noted: i) the lines involving a $J = 2$ level are not as broad as in the ν_2 case, ii) there is no evidence of a RTC structure as observed for ν_2.

This could be explained by a coupling of the rotation-vibration to the translation in the cage weaker for the stretching modes ν_1, ν_3 than for the bending mode ν_2.

Some dimeric species are also observed in this frequency range. The measured frequencies (see Table 3) are in good agreement with the literature [16].

6. Double doping experiments with CO_2: the complex

H_2O *frequency ranges*

To look at the H_2O:CO_2 complex near H_2O absorptions, the sample should be concentrated in CO_2 [19]. However, as CO_2 has a great tendency to form polymers, its concentration should be kept low enough to avoid aggregates of H_2O with more than one CO_2 molecule. In Fig. 4, we can compare typical spectra obtained with a sample of pure H_2O (spectrum P — $H_2O/A = 1/500$) to spectra of CO_2 double doped samples (spectra D_1 — $H_2O/CO_2/Ar = 10/5/5000$ and D_2 — $H_2O/CO_2/Ar = 10/2/5000$), recorded with 0.03 cm^{-1} resolution. The spectra were recorded at 6 K, after an annealing at 30 K, which enhances the complex absorptions. Some new lines appear in the double doped experiment due to the simultaneous presence of H_2O and CO_2. As the dilutions remain high enough, there is a weak probability of trimolecular species. With the H_2O dimer absorptions, for the H_2O:CO_2 complex, the most intense narrow structures which can be measured are indicated in Table 3. By varying the relative concentration of CO_2, we have checked that the behavior of these lines is consistent with a 1:1 pair, as they grow proportionally with the concentration of CO_2 for a given concentration of H_2O. Our results are compared in Table 3 with the recent ones of Svensson et al. [24].

Table 3

Most intense observed lines (cm^{-1}) of H_2O dimer and H_2O:CO_2 complex isolated in solid argon

Line	H_2O:H_2O		H_2O:CO_2	
	This work	Perchard [16]	This work	Svensson et al. [24]
H_2O (v_1)	3574.77 3633.22	3574.0 (PD) 3633.1 (PA)	3638.0	3632.7
H_2O (v_2)	1592.94 1610.12	1593.1 (PA) 1610.6 (PD)	1589.48 1589.86 1590.54	1593.1
H_2O (v_3)	3708.5 3738.1	3708.0 (PD) 3715.7 (PA) 3737.8 (PA)	3732.46	3732.9
CO_2 (v_2)			656.03 667.95 668.05	656.0 668.0
CO_2 (v_3)			2340.20	2340.5

PA: proton acceptor; PD: proton donor.

In the H_2O ν_1 range, beside the combination bands ($2\nu_2+\nu_3$) of CO_2 reported by Schriver et al. [25] around 3596.9 and 3602.98 cm^{-1}, only a weak line due to the double presence of H_2O and CO_2 can be de-

tected at 3638 cm^{-1}. Near ν_2, two clear structures appear at 1589.48 cm^{-1}, with shoulders at 1589.04 and 1589.81 cm^{-1} and a narrower line at 1589.86 cm^{-1}. The broad and weak absorptions around 1591.5 and 1591.8 cm^{-1} are also due to the presence of CO_2. The spectra, for the ν_3 mode, exhibit clearly a broader absorption at 3732.46 cm^{-1} close to the combination bands ($\nu_1+\nu_3$) of CO_2 [25].

The number of these absorptions, especially for the ν_2 mode of H_2O, is probably due to multiple trapping sites for the complex and different geometries, as the vibrational modes of H_2O are not degenerate. The broad structures could be due to very perturbed crystalline double cages.

CO_2 *frequency ranges*

In typical experiment presented in Fig. 5, the samples are more dilute in CO_2 (spectra P: CO_2/Ar = = 1/5000 and D: $CO_2/H_2O/Ar$ = 1/10/5000). The striking new features are: one narrow structure at 668.05 cm^{-1} (with a shoulder at 667.95 cm^{-1}), a much weaker broad one at 656.03 cm^{-1} in the ν_2 range, and one narrow line at 2340.20 cm^{-1} in the ν_3 range. These results are consistent with those reported in the literature [24]. We should mention that the line at 2340.2 cm^{-1} had already been assigned to this complex by Guasti et al. [26] in 1978, in experiment on CO_2 in solid argon, for which an amount of water was present due to a leak in the system.

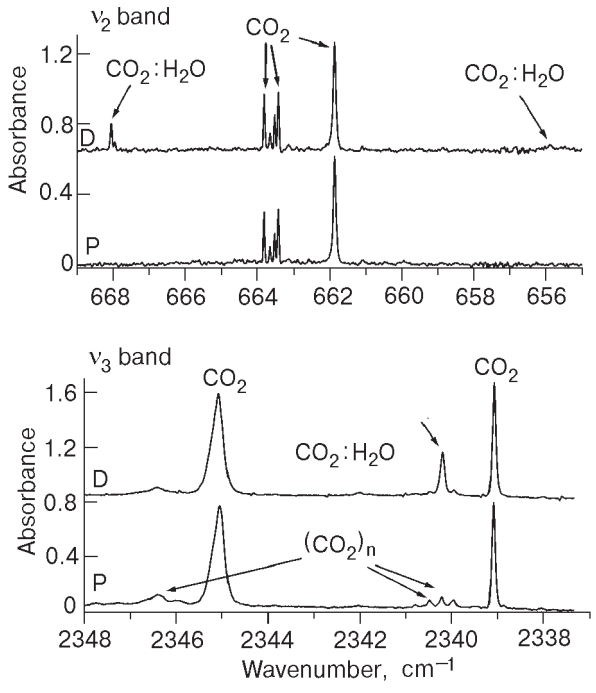

Fig. 5. Double doping with CO_2: carbon dioxide regions at 6 K. The spectra are recorded with 0.03 cm^{-1} resolution, after annealing at 30 K; P is a pure CO_2 sample (CO_2/Ar = = 1/5000, thickness ~ 60 μm) and D is a double doped sample ($H_2O/CO_2/Ar$ = 1/10/5000, thickness ~ 60 μm).

7. Conclusion

Our new experimental data has led to some new assignments of the rovibrational frequencies of H_2O on the ν_2 mode, and the absorptions of the H_2O:CO_2 complex in the H_2O regions in argon matrix. From our refined measurements of rovibrational frequencies, the «effective» rotational constants of water trapped in solid argon may be determined. Furthermore, our experimental results will support calculations able to explain the RTC structure. For the complex with CO_2, some more experimental work is needed to understand the different trapping sites and structures. A modeling similar to that developed for the CO:CO_2 complex [27] will be attempted.

Acknowledgments

The authors acknowledge Louise Schriver-Mazzuoli for helpful discussions.

1. L.S. Rothman, C.P. Rinsland, A. Goldman, S.T. Massie, D.P. Edwards, J.M. Flaud, A. Perrin, C. Camy-Peyret, V. Dana, J.Y. Mandin, J. Schroeder, A. McCann, R.R. Gamache, R.B. Wattson, K. Yoshino, K.V. Chance, K.W. Jucks, L.R. Brown, V. Nemtchinov, and P. Varanassi, *J. Quant. Spectrosc. Radiat. Transfer* **60**, 665 (1998).
2. L.R. Brown, R.A. Toth, and M. Dulick, *J. Mol. Spectrosc*. **212,** 57 (2002).
3. P.F. Coheur, S. Fally, M. Carleer, C. Clerbaux, R. Colin, A. Jenouvrier, M.F. Merienne, C. Hermans, and A.C. Vandaele, *J. Quant. Spectrosc. Radiat. Transfer* **74**, 493 (2002).
4. C. Lobban and J.L. Finney, *J. Chem. Phys*. **112**, 7169 (2000).
5. L. Schriver-Mazzuoli, A. Schriver, and A. Hallou, *J. Mol. Struc*. **554**, 289 (2000).
6. V.P. Dmitriev, S.B. Rochal, and P. Toledano, *Phys. Rev. Lett*. **71**, 553 (1993).
7. D. Prialnik and Y. Mekler, *Astrophys. J.* **366**, 318 (1991).
8. A. Coustenis, A. Salama, E. Lellouch, Th. Encrenaz, G.L.Bjoraker, R.E. Samuelson, Th. de Graauw, H. Feuchtgruber, and M.F. Kessler, *Astron. Astrophys*. **336,** L85 (1998).
9. L.B. d'Hendecourt and M. Jourdain de Muizon, *Astron. Astrophys.* **223,** L5 (1989).
10. L. Fredin, B. Nelander, and G. Ribbegard, *Chemica Scripta* **7,** 11 (1975).

11. P. Ehrenfreund, A.C.A. Boogert, P.A. Gerakines, A.G.G.M. Tielens, and E.F. van Dishoeck, *Astron. Astrophys*. **328**, 649 (1997).
12. J.A. Glasel, *J. Chem. Phys*. **33**, 252 (1960).
13. R.L. Redington and D.E. Milligan, *J. Chem. Phys*. **39**, 1276 (1963).
14. R.M. Bentwood, A.J. Barnes, and W.J. Orville-Thomas, *J. Mol. Spectrosc*. **34**, 391 (1980).
15. A. Engdahl and B. Nelander, *J. Mol. Struct*. **193**, 101 (1989).
16. J.P. Perchard, *Chem. Phys*. **273**, 217 (2001).
17. D. Forney, M.E. Jacox, and W.E. Thompson, *J. Mol. Spectrosc*. **157**, 479 (1993).
18. D. Jasmin, P. Brosset, R. Dahoo, B. Gautier-Roy, and L. Abouaf-Marguin, *J. Chem. Phys*. **108**, 2302 (1998).
19. V. Raducu, D. Jasmin, R. Dahoo, P. Brosset, B. Gauthier-Roy, and L. Abouaf-Marguin, *J. Chem. Phys.* **101**, 1878 (1994).
20. V. Raducu, D. Jasmin, R. Dahoo, P. Brosset, B. Gauthier-Roy, and L. Abouaf-Marguin, *J. Chem. Phys*. **102**, 9235 (1995).
21. B. Gauthier-Roy, L. Abouaf-Marguin, and P. Boissel, *J. Chem. Phys*. **98**, 6827 (1993) and references therein.
22. X. Michaut, A.M. Vasserot, and L. Abouaf-Marguin, to be published.
23. H. Friedmann and S. Kimel, *J. Chem. Phys*. **47**, 3589 (1967).
24. T. Svensson, B. Nelander, and G. Karltrom, *Chem. Phys*. **265**, 323 (2001).
25. A. Schriver, L. Schriver-Mazzuoli, and A.A. Vigasin, *Vib. Spectrosc*. **23**, 83 (2000).
26. R. Guasti, V. Schettino, and N. Brigot, *Chem. Phys*. **34**, 391 (1978).
27. J. Langlet, J. Caillet, M. Allavena, V. Raducu, B. Gauthier-Roy, R. Dahoo, and L. Abouaf-Marguin, *J. Mol. Struct*. **484**, 145 (1999).